Using Mobile Phones as Acoustic Sensors for High-throughput Surveillance of Mosquito Ecology

Haripriya Mukundarajan,[1] Felix JH Hol,[2] Erica A Castillo,[1]
Cooper Newby,[1] Manu Prakash[2*]
[1]Department of Mechanical Engineering, Stanford University,
[2]Department of Bioengineering, Stanford University
Stanford, CA 94305, USA
*To whom correspondence should be addressed; E-mail: manup@stanford.edu.

The lack of high-resolution field data on the abundance, species and distribution of mosquitoes is a serious impediment to effective control of mosquito-borne disease, yet the availability of high-throughput, low-cost surveillance techniques remains a bottleneck in generating such data. Here, we establish that commercially available mobile phones (including low-cost basic models) are a powerful tool to probe mosquito activity, by sensitively acquiring acoustic data on their species-specific wingbeat sounds, together with the time and location of the human-mosquito encounter. We survey a range of medically important mosquito species to quantitatively demonstrate how acoustic recordings supported by spatio-temporal metadata enable rapid, non-invasive species identification. As proof-of-concept, we carry out field demonstrations where minimally-trained users map local mosquito fauna using their personal phones. Thus, by leveraging the global mobile phone infrastructure with the potential for engaging citizen scientists, our approach enables continuous large-scale acquisition of mosquito surveillance data in resource-constrained areas.

Frequent, widespread, and high resolution surveillance of mosquitoes is essential to understanding their complex ecology and behaviour (*1, 2*), in order to predict disease risk and formulate effective control strategies against mosquito-borne diseases like malaria, dengue and Zika (*3, 4*). Mosquito populations vary heterogeneously across urban and rural landscapes, further fluctuating with seasonal or climatic trends and human activities. Hence, the direct monitoring of mosquito species and abundance in field settings is necessary to shape appropriate and timely vector control measures (*5, 6*). Yet, a paucity of such ecological data continues to remain a significant bottleneck in disease control efforts, particularly in resource-poor areas, since current surveillance techniques such as trapping and manual identification are labour, time, and cost intensive. Consequently, although there have been extensive efforts to map mosquito abundance using interpolative mathematical models, their field inputs from entomological surveys are comparatively sparse (*7*). Therefore, there is a crucial need for novel methods of surveillance that are extremely low-cost yet high-throughput, to adequately sample mosquito populations across large areas while simultaneously maintaining high spatio-temporal resolutions.

A promising candidate to answer this need is acoustic monitoring, where the wingbeat sounds produced by mosquitoes in flapping-wing flight are used to identify different species in the field (*8–12*). This is based on the hypothesis that sexual selection has led to unique species-specific sound signatures for different mosquito species (*13–18*). However, the challenges of using expensive microphones to acquire low amplitude mosquito sounds against potentially high background noise levels pose a barrier to the widespread adoption of acoustic surveillance as a field technique (*19–21*). Low-cost technologies using optical measurement as a proxy for sound are promising in overcoming such limitations (*22–25*). Yet, the global scalability of such a specific hardware-based solution remains a challenge for large-scale deployment.

Here, we propose a novel solution that uses mobile phones to enable widespread acoustic mosquito surveillance, by using them as sensitive microphones to record species-specific wingbeat sounds from a variety of disease-transmitting mosquitoes for identification and analysis (Fig. 1A). We exploit the insight that these ubiquitous, highly portable devices are optimized for sophisticated audio processing and computing capabilities, and connected by a data transmission infrastructure supporting over 5 billion users globally (*26*), leading to multiple applications in citizen science and crowdsourced data gathering (*27–30*). Specifically, the explosive growth in mobile phone use is most pronounced in Africa, Asia and Latin America (*26*), which also bear the brunt of the impact of mosquito-borne disease (*2*). This juxtaposition implies that our mobile phone based concept has the advantages of scalability, sustainability and cost effectiveness, in collecting on-the-ground data on mosquito activity in resource-constrained areas with high disease burdens. Our proof-of-concept study highlights the potential of our solution to engage citizen scientists around the world in mosquito surveillance, without the need for specialized equipment or highly trained personnel.

We acquire acoustic signatures from free flying mosquitoes by orienting the primary microphone of a mobile phone in the direction of a mosquito, and using an in-built audio recording application to record and store the sound produced by the mosquito's wingbeats (Fig. 1A,B, Supplementary Audio SA1). Mosquito sounds have relatively low complexity, comprising a single fundamental frequency with several overtones, which we extract using the short time Fourier transform (STFT) (Fig. 1C). These sounds are sexually dimorphic with males having higher frequencies than females, and show natural variations in the fundamental frequency which are captured by a base frequency distribution characteristic of the given species (Fig. 1D). The female wingbeat frequency is typically between 200 to 700 Hz, which overlaps the voice band (300 to 3000 Hz) in which phones are designed to have maximum sensitivity. Since

mosquitoes rarely fly at speeds over half a meter per second, the Doppler shift of frequency during free-flight is small ($1 - [330 - 0.5/330 + 0.5] \approx 0.3\%$, i.e. < 2 Hz) when compared to the observed natural spreads of up to 100 Hz in base frequency distributions. The use of mobile phones as recording platforms additionally provides automatic registration of relevant metadata, such as the location and time of data acquisition, which adds valuable secondary information for species identification and spatio-temporal mapping. Such acoustic and spatio-temporal information can be crowdsourced from many users, to generate large data sets that map the distribution of mosquito species at high resolutions (Fig. S1).

To establish our fundamental premise that mobile phone microphones are indeed high fidelity acoustic sensors, we first assessed whether mobile phones faithfully record the spectral composition of sound produced by mosquito wings during flight. We measured the wingbeat frequency of female *Culex tarsalis* mosquitoes in tethered flight using two independent modalities, by synchronizing acoustic recordings with high speed videography (Fig. 2A). For spectrograms derived from mobile phone audio (Sony Xperia Z3 Compact) and high speed video recordings, and aligned in time to within 2 ms, we find an exact match in frequency in each time window to within a computational error margin of 2 Hz (Fig. 2B). The respective distributions of the base frequency have low variances with maximum density occurring in the same bin (Fig. 2C), and are indistinguishable by the 2-sample T-test (significance level $\alpha = 1\%$). This corroborates the spectral accuracy of mobile phone recordings based on an independent optical reference standard.

As we propose using mobile phones as wingbeat acoustic sensors under field conditions, it is crucial to establish working limits within which their built-in microphones are sensitive enough to reliably acquire low amplitude mosquito sounds. Since the technical specifications

of many commercially available mobile phone microphones are not openly available, we experimentally compared a range of mobile phone models having diverse feature capabilities to two reference electret condenser microphones under identical conditions. This provides a direct comparison of mobile phone microphones to the gold standard in acoustic sensing. We first used a piezoelectric buzzer of constant amplitude (77 dB at source) and frequency (500 Hz) as a standardized sound source, to show that both smartphones (iPhone 4S, Xperia Z3 Compact) and low-end feature phones (SGH T-209 clamshell model) had signal-to-noise ratios (SNR) that were comparable to the reference microphones over distances of up to 100 mm (Fig. 2D). Next, to gauge suitable working distances for the specific application of acquiring mosquito sound, we simultaneously recorded wingbeat sound from tethered mosquitoes using the reference microphones and mobile phones. Curves of mobile phone SNR over distance indicate that all the phones tested, including a decade-old basic phone (SGH T-209), are capable of acquiring detectable wingbeat sound up to at least 50 mm from a mosquito (Fig. 2E). This is a working distance that we have found to be practically achievable with reasonable ease when making free-flight measurements in the field. Smartphones like the Xperia are capable of signal detection even at up to 100 mm in quiet environments, making it still easier for users to record mosquitoes (Fig. S2).

For our proposed surveillance technique to scale to the broadest possible user base, citizen scientists must be able to engage in acoustic data collection using any commercially available mobile phone that they own. The varying sensitivity observed among phone models highlights the imperative that most mobile phones should still collect quantitatively comparable acoustic data from mosquitoes. We tested this for a collection of eight different commercially available cellphones (Fig. 2F, ranging in price from $\sim$ \$20 to $\sim$ \$700), where female mosquitoes of similar age from a lab-reared population of the malaria vector *Anopheles stephensi* were con-

fined in a cage, and recorded by manually following them in free-flight. Quantitatively, both mean and median frequencies obtained by each phone lie well within the interquartile range of frequencies obtained by every other phone, and differ by less than 5% of each other (Fig. 2F). The distributions of wingbeat frequency all have high degrees of mutual overlap, as measured by Bhattacharya overlap distances (BD) between 0.93 to 1 (Fig. 2H). We further computed the Jensen-Shannon divergence metric (JSD) between each pair of phones (Fig. 2G), which had low values below 0.3 corroborating that wingbeat frequency sampling is relatively insensitive to the phone used. Thus, our data demonstrate that a diverse range of both smart and feature phones provide highly similar acoustic spectra from the same population of mosquitoes, as required of a truly universal platform for crowdsourcing mosquito identification via audio signal acquisition. Further, the JSD also provides upper bounds on the variation inherent in sampling the same population in different experiments, allowing us to establish a criterion for the minimum statistical distances required between wingbeat frequency distributions of different species in order to distinguish them.

The difference between wingbeat frequency distributions among mosquito species has a profound impact on the probability of correct species identification in acoustic surveillance (*24, 25, 31, 32*). To evaluate this, we carried out a broad survey of frequency distributions for lab-reared populations of female mosquitoes from 19 major mosquito vector species under similar experimental conditions (Fig. 3A). Our analysis is exclusively based on free-flight acoustic data acquired by the 2006-model SGH T-209 feature phone ($\sim$ \$20), to demonstrate the capacity for acoustic identification using a low-end phone with very basic functionality. The vast majority of all possible pairwise combinations of species in our study (184 out of 190) had JSD greater than the maximum value of 0.3 for different samples of the same species computed earlier in Fig. 2G, indicating that acoustic differences between species are typically significantly

greater than the variations in sampling a single species using different phones (Fig. 3B).

We explored our species survey data in depth to identify different scenarios where acoustic data from mobile phones can be combined with automatically registered metadata such as timestamps and location coordinates, to facilitate quick differentiation between common medically relevant vector species in the field (Fig. 3C,S3). In the simplest cases, species with completely non-overlapping frequency distributions, such as *Anopheles gambiae* and *Culex pipiens* (JSD $= 1$), can easily be distinguished by sound alone (Fig. S3A). Although some species in our large dataset (Fig. 3A) have overlapping frequency distributions, location metadata from the phone allows us to overlook these pairs on the basis of spatial distribution, such as the European *An. atroparvus* and South Asian *An. dirus* (JSD $= 0.26 < 0.3$) (*33*) (Fig. S3B). Other pairs of species overlapping in both frequency and spatial distribution can be distinguished by metadata such as timestamps (*24, 25*), for instance the night-biting *An. gambiae* and day-biting *Aedes aegypti* (JSD $= 0.37 \sim 0.3$) (Fig. S3C). Co-occurring and highly similar species that are reasonably distinguishable acoustically include the arboviral vectors *Ae. aegypti* and *Ae. albopictus* (JSD $= 0.55 > 0.3$) (*31*), and the closely related species *Cx. pipiens* and *Cx. quinquefasciatus* (JSD $= 0.65 > 0.3$) (Fig. S3D). Morphologically indistinguishable vector species like the *Anopheles gambiae s.l.* complex are of particular interest for acoustic identification (*32, 34, 35*). Our results for four members of this complex imply partial distinguishability, based on mostly mutually non-overlapping interquartile ranges for *An. arabiensis*, *An. quadriannulatus*, *An. gambiae* and *An. merus*, with JSD for all but one species pair ranging between 0.61 and 0.91 (Fig. S3E). However, the pair of *An. arabiensis* and *An. merus* is potentially indistinguishable (JSD $= 0.29 < 0.3$) (Fig. S3F) without additional knowledge of their specific local ecology, such as the distribution of saltwater breeding sites for the halophilic *An. merus*. Nevertheless, despite a very few limiting cases, the broadly species specific nature of acoustic data, combined

with the discriminatory power of phone provided time and location metadata, makes mobile phone based acoustic surveillance an extremely useful screening tool to gain broad insights into mosquito populations at a glance (Fig. 3C).

To demonstrate the efficacy of acoustic surveillance using mobile phones in the field, we collected data in a variety of settings from urban to rural, both indoors and outdoors. We recorded acoustic signatures from mosquitoes that were either free-flying, taking off from rest, or captured in inflated Ziploc bags (Fig. S4, Supplementary Audio SA2-7). The high amplitude and distinctive narrow-spectrum characteristics of mosquito sounds allowed us to easily identify them within spectrograms, as the SNR remained high due to manual control of microphone position and orientation relative to the mosquito. These sound signatures were matched against our frequency distribution database (Fig. 3A, data for males not shown) to identify the respective species, which we also confirmed by capturing the respective specimens for morphological identification by optical microscopy. Such field data also allowed us to explore variations in wingbeat frequency among mosquitoes exhibiting considerable variations in body size and wingspan within the same species (Fig. 3D,E). Despite the dependence of wingbeat frequency on factors such as nutrition, age, temperature (*36*) and size (*34*), our treatment of this measurement as a distribution over time rather than a single discrete value allows greater comparability between individuals of a given species. Interestingly, in field recordings of *Ochlerotatus sierrensis* mosquitoes varying almost two-fold in size (Fig. 3E), the difference in mean frequency between each specimen was about the same as the inter-quartile range for individual flight traces obtained from a single mosquito (Fig. 3D). This indicates that frequency variations within flight sequences of several seconds - perhaps due to aerial maneuvers - may contribute as much to the widening of frequency distributions as do variations between individuals. Thus, wingbeat frequency can be a robust identifying characteristic for different species in the field, when treated

as a distribution over time for longer flight traces of a few seconds.

Finally, we assessed the feasibility of our approach for spatio-temporal mapping of mosquitoes in the field through citizen science, with small-scale proof-of-concept field trials carried out at Ranomafana village in Madagascar (RNM) and Big Basin Redwoods State Park in California, USA (BBR). First, we acquired curated acoustic signatures associated with morphologically identified specimens of the local mosquito fauna caught in traps (Fig. 4A,B). This subsequently formed the basis for acoustic identification of mobile phone recordings in the field, collected by 8 to 15 volunteers using their personal mobile phones, who were given around 15 minutes of training in acoustic data collection (sample field recordings in Supplementary Audio SA8-10). In the maps constructed using this field data (Fig. 4C,D), the power of crowdsourcing in comparison to many traditional surveillance techniques is reflected both in the volume of data per time (~ 60 recordings over 3 hours in RNM, comparable to the number collected overnight in a CDC light trap at the same location; ~ 125 recordings over 3 hours in BBR), and also the spatio-temporal fine-graining on the level of minutes and tens of meters. In the multi-species ecology of RNM, complementary gradients in the density of each species were evident across the village from riverside to hillside, possibly influenced by extremely local factors such as drainage, density of humans, or presence of livestock (Fig. 4C). Spatial variations in mosquito population density were clearly seen even for the single species that dominated the relatively uniform terrain of BBR (Fig. 4D), and parsing of the data by recording time further revealed the rise and fall in biting activity over an evening (Fig. 4D inset). These pilot field trials highlight the extremely local variations in mosquito distributions together with their circadian activity patterns. This indicates that mobile phone based crowdsourcing for mosquito surveillance is uniquely equipped to simultaneously optimize both scale and resolution of ecological measurements for the spatiotemporal mapping of mosquito vectors.

In summary, we have demonstrated a method for acoustic surveillance of mosquitoes using mobile phones, by presenting quantitative analyses of mobile phone acoustic signal quality and differentiation between mosquito species, further supported by preliminary field data collected by volunteers and organized into spatio-temporal maps. The involvement of local volunteers in our study underlines that almost anyone with a mobile phone can quickly be trained to contribute data towards mosquito surveillance efforts. With the proof-of-concept presented here, we highlight the potential for building high-density mosquito maps with the participation of citizen scientists, particularly in disease-prone locations where high human population density coincides with complex mosquito ecology. The advent of machine learning and data mining techniques create tremendous scope for the automated processing of crowdsourced acoustic mosquito surveillance data (*24, 25*). This could boost our capability to dynamically assess mosquito populations, study their connections to human and environmental factors, and develop highly localized strategies for pre-emptive mosquito control (*37*). Since the critical missing link in enabling such advances at present is the capacity to generate large quantities of mosquito ecological data on fine-grained space and time scales (*4*), our mobile phone based solution holds great promise as a scalable, non-invasive, high-throughput and low-cost strategy to generate such data, by leveraging widely available hardware and an existing network infrastructure. Thus, we propose a citizen science effort driven by the mobile phone based mapping framework established in this study (Fig. S1), which will enable people to take the initiative in tracking disease vectors within their own communities, expand surveillance efforts in resource-limited areas where they are needed the most, and bring about new big data driven approaches for eliminating vector-borne disease.

References

1. G. Macdonald, *Bulletin of the World Health Organization* **15**, 613 (1956).

2. World Health Organization, A global brief on vector-borne diseases. (2014).

3. H. Townson, *et al.*, *Bulletin of the World Health Organization* **83**, 942 (2005).

4. H. M. Ferguson, *et al.*, *PLoS Med* **7**, 1 (2010).

5. H. C. J. Godfray, *Journal of Animal Ecology* **82**, 15 (2013).

6. N. J. Besansky, *Current Opinion in Insect Science* **10**, 201 (2015).

7. S. I. Hay, *et al.*, *PLoS Med* **7**, e1000209 (2010).

8. M. C. Kahn, W. Celestin, W. Offenhauser, *et al.*, *Science* **101**, 335 (1945).

9. M. C. Kahn, W. Offenhauser Jr, *American Journal of Tropical Medicine* **29**, 811 (1949).

10. W. H. Offenhauser, M. C. Kahn, *The Journal of the Acoustical Society of America* **21**, 259 (1949).

11. M. C. Kahn, W. Offenhauser, *The American Journal of Tropical Medicine and Hygiene* **29**, 827 (1949).

12. B. J. Johnson, S. A. Ritchie, *Journal of medical entomology* **53**, 245 (2016).

13. P. Belton, *Journal of the American Mosquito Control Association* **10**, 297 (1994).

14. G. Gibson, I. Russell, *Current Biology* **16**, 1311 (2006).

15. L. J. Cator, B. J. Arthur, L. C. Harrington, R. R. Hoy, *Science* **323**, 1077 (2009).

16. B. Warren, G. Gibson, I. J. Russell, *Current Biology* **19**, 485 (2009).

17. C. Pennetier, B. Warren, K. R. Dabiré, I. J. Russell, G. Gibson, *Current Biology* **20**, 131 (2010).

18. L. J. Cator, K. R. Ng'Habi, R. R. Hoy, L. C. Harrington, *Behavioral Ecology* **21**, 1033 (2010).

19. M. Jones, *Journal of Insect Physiology* **10**, 343 (1964).

20. D. Unwin, C. Ellington, *Journal of Experimental Biology* **82**, 377 (1979).

21. D. R. Raman, R. R. Gerhardt, J. B. Wilkerson, *Transactions of the ASABE* **50**, 1481 (2007).

22. A. Moore, J. R. Miller, B. E. Tabashnik, S. H. Gage, *Journal of economic entomology* **79**, 1703 (1986).

23. G. E. Batista, E. J. Keogh, A. Mafra-Neto, E. Rowton, *Proceedings of the 17th ACM SIGKDD international conference on Knowledge discovery and data mining* (ACM, 2011), pp. 761–764.

24. Y. Chen, A. Why, G. Batista, A. Mafra-Neto, E. Keogh, *Journal of insect behavior* **27**, 657 (2014).

25. D. F. Silva, V. M. A. Souza, D. P. W. Ellis, E. J. Keogh, G. E. A. P. A. Batista, *Journal of Intelligent & Robotic Systems* **80**, 313 (2015).

26. P. Cerwall, *et al.*, *Ericsson.[Online]. Available.: www. ericsson. com/res/docs/2015/ericsson-mobility-report-june-2015. pdf [June 2015]* (2015).

27. E. A. Graham, S. Henderson, A. Schloss, *Eos, Transactions American Geophysical Union* **92**, 313 (2011).

28. C. L. Catlin-Groves, *International Journal of Zoology* **2012**, 349630 (2012).

29. E. Malykhina, *Scientific American* (2013).

30. Q. Kong, R. M. Allen, L. Schreier, Y.-W. Kwon, *Science advances* **2**, e1501055 (2016).

31. W. G. Brogdon, *Journal of medical entomology* **31**, 700 (1994).

32. W. G. Brogdon, *Journal of medical entomology* **35**, 681 (1998).

33. M. E. Sinka, *et al.*, *Parasites & vectors* **5**, 69 (2012).

34. J. Wekesa, W. Brogdon, W. Hawley, N. Besansky, *Physiological entomology* **23**, 289 (1998).

35. F. Tripet, G. Dolo, S. Traoré, G. C. Lanzaro, *Journal of medical entomology* **41**, 375 (2004).

36. J. Oertli, *Journal of experimental biology* **145**, 321 (1989).

37. S. I. Hay, D. B. George, C. L. Moyes, J. S. Brownstein, *PLoS med* **10**, e1001413 (2013).

We acknowledge Amalia Hadjitheodorou, members of the Prakash Lab, and data collection volunteers for assistance in field experiments, and Mainak Chowdhury for inputs regarding analysis of the data. We particularly thank Menja Brabaovola and Malalatiana Rasoazanany for their invaluable participation in field studies in Madagascar. We are grateful to Ellen Dotson and Mark Benedict at the US Centres for Disease Control, the Luckhart and Coffey labs at UC Davis, the Zohdy and Mathias labs at Auburn University, and the Animal Flight Lab at UC Berkeley, for providing us with access to their mosquito cultures for collecting audio data. We further acknowledge Big Basin Redwoods State Park, California, USA, where we collected acoustic signatures of mosquitoes on hiking trails. We are thankful to the Centre ValBio in Ranomafana, Madagascar for enabling our field studies in the area, and to PIVOT and particularly Andrés Garchitorena for coordinating our field based efforts. We are

grateful to Nona Chiariello and the Jasper Ridge Biological Preserve at Stanford University, the Santa Clara County Vector Control District and the San Mateo County Mosquito Control District for their support and assistance with providing access for field work, materials for cultures, and assisting with identification of field specimens. The materials for cultures in our lab were provided by BEI Resources and NIAID. Finally, we thank Desirée LaBeaud, Erin Mordecai, John Dabiri, and all members of the Prakash Lab for illuminating discussions about our work and comments on our manuscript.

HM acknowledges support from a HHMI International Student Research Fellowship, EAC from a Stanford Mechanical Engineering Graduate Fellowship, and FH from a NWO Rubicon Fellowship. MP acknowledges support from the NSF Career Award, HHMI-Gates Faculty Fellows program, the Pew Foundation Fellowship and the MacArthur Fellowship. This work was additionally supported by the Coulter Foundation, the Woods Environmental Institute at Stanford University, the NIH New Innovator Grant and the USAID Grand Challenges : Zika and Future Threats award.

The authors declare that they have no competing financial interests.

Fig. 1. Mobile phone users can collect acoustic data from mosquitoes characterized by the base frequency and harmonics.

A, Illustration showing the collection of mosquito acoustic data by mobile phone users in different locations. **B**, Methods to acquire wingbeat sounds from mosquitoes using mobile phones include lab methods like (i) collecting them in cages, and field methods like (ii) following mosquitoes in free-flight, or (iii) capturing them in inflated bags. **C**, Spectrogram for a flight trace acquired from an individual female *Anopheles gambiae* mosquito using a 2006 model Samsung SGH T-209 flip phone. The wingbeat base frequency at every instant is computationally identified by a simple automated algorithm and marked with a black line. (Top) The time-averaged spectrum of this flight trace shows the distribution of acoustic power among the base frequency and multiple harmonics. **D**, The variations in wingbeat base frequency of the mosquito during this flight trace are represented by a probability distribution of the frequency identified in each window of the spectrogram. (Top) Raw base frequency data is represented as a violin plot with an overlaid box plot marking the inter-quartile range, black circle representing mean frequency, gray vertical bar for median frequency, and whiskers indicating 5th and 95th quantiles.

Figure 1: Mobile phone users can collect acoustic data from mosquitoes characterized by the base frequency and harmonics

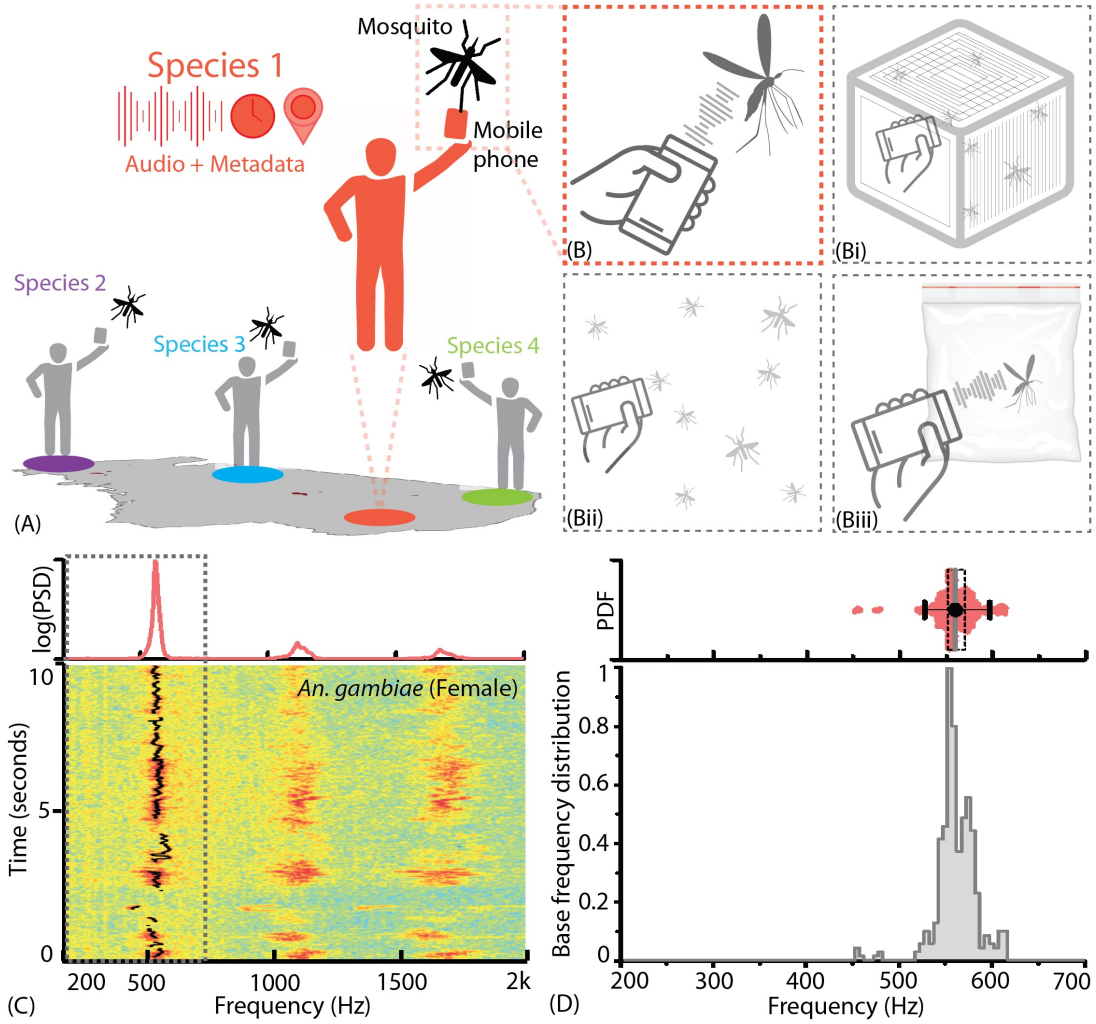

Fig. 2. Mobile phones sensitively acquire high fidelity acoustic data from mosquitoes with comparable performance across models

A, Schematic of experimental setup for recording a tethered mosquito using mobile phones, with synchronized high speed cameras or high performance microphones as visual and auditory reference standards. Synchronization on the order of microseconds is achieved using a piezo-electric buzzer and LED controlled by a microprocessor. **B**, Overlaid spectrograms for female *Culex tarsalis* mosquitoes obtained independently using high speed video (magenta) and mobile phone audio (cyan), aligned to within 2 ms and showing a spectral overlap (blue) within 2 Hz across all time instances. The mobile phone data is noisy but faithfully reproduces the base frequency peak of 264 Hz and the first two overtones. **C**, Base frequency distributions from video and audio are indistinguishable by the 2-sample T-test ($n = 165$, $\alpha = 1\%$). **D**, Signal-to-noise ratio (SNR) estimates over distance from a standardized sound source show that mobile phone microphone performance within a 100mm radius is superior or comparable to high performance studio microphones. **E**, SNR over distance for the wingbeat sound produced by a tethered female *Cx. tarsalis* mosquito (normalized for a source amplitude of 45 dB), provide working limits where phones can detect the audio signal - 50 mm for the low end T-209 feature phone and 100 mm for the iPhone 4S and Xperia Z3 Compact smartphones. **F**, Variation of the base frequency distribution sampled by 8 different phones is low compared to the natural variation within a population of about 200 lab-reared *Anopheles stephensi* females. Raw data are shown with overlaid box plots marking the inter-quartile range, black circles for mean frequency, gray vertical bars for median frequency, and whiskers indicating 5th and 95th quantiles. **G,H**, The Jensen-Shannon divergence metric for base frequency distributions (**G**, lower left triangle) shows low disparity, ranging between 0.144 and 0.3, against a minimum of 0 for identical distributions. Likewise, the Bhattacharya distance (**H**, upper right triangle) shows high overlap, with values between 0.935 to 0.986, against a maximum of 1 for identical distributions.

Figure 2: Mobile phones sensitively acquire high fidelity acoustic data from mosquitoes with comparable performance across models

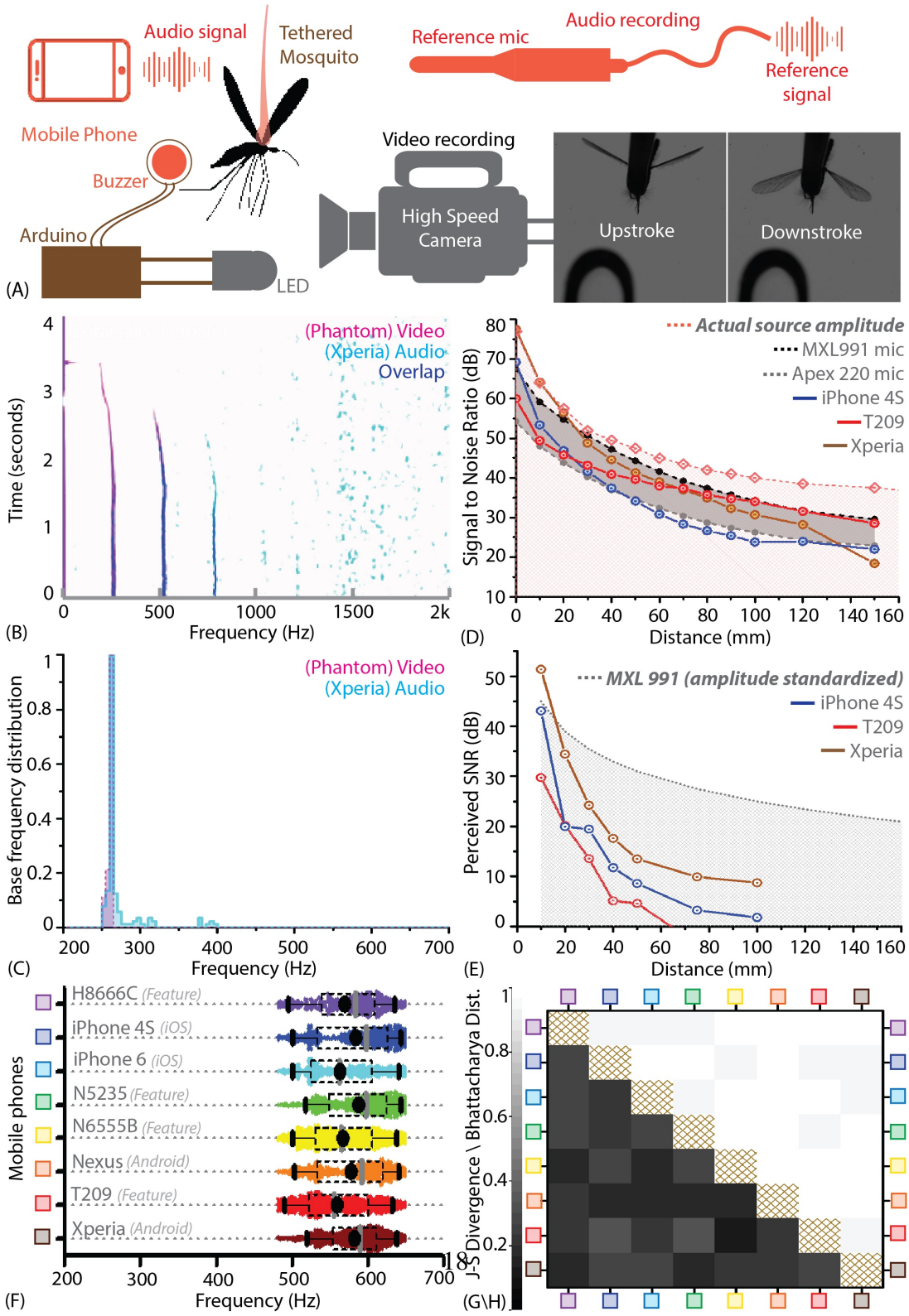

Fig. 3. Mosquitoes of different species are distinguishable based on base frequency distributions and spatio-temporal metadata

A, Distribution of base frequencies for lab-reared female mosquitoes of 19 medically relevant species, for recordings obtained with the 2006 model T-209 low-end feature phone (except *Cu. incidens*, *Cx. pipiens* and *Cx. quinquefasciatus*, recorded using iPhone models). **B**(lower left triangle), Jensen-Shannon divergence metric for base frequency distributions. Distributions are spaced apart with high J-S divergence in most cases, with only four pairwise combinations having J-S divergence around 0.3 - the maximum divergence for the same species across different phones. **C** (upper right triangle), Classifiation of species pairs according to the possibility of distinguishing them using mobile phones — (i) no frequency overlaps, hence distinguishable by acoustics alone, (ii) overlapping frequency distributions, but not geographically co-occurring hence distinguishable using location, (iii)overlapping frequency distributions but distinguishable using time stamps, (iv) partially overlapping frequency distributions but no location-time distinctions, hence distinguishable but not in all cases, (v) indistingishable due to highly overlapping frequency distributions with co-occurrence in space and time. **D,E**, Variations in base frequency distribution **(D)** for field-recorded sounds corresponding to wild mosquitoes having a wide (about two-fold) variation in body size and wing area **(E)**, showing small differences between individuals compared to the variation within each flight trace.

Figure 3: Mosquitoes of different species are distinguishable based on base frequency distributions and spatio-temporal metadata

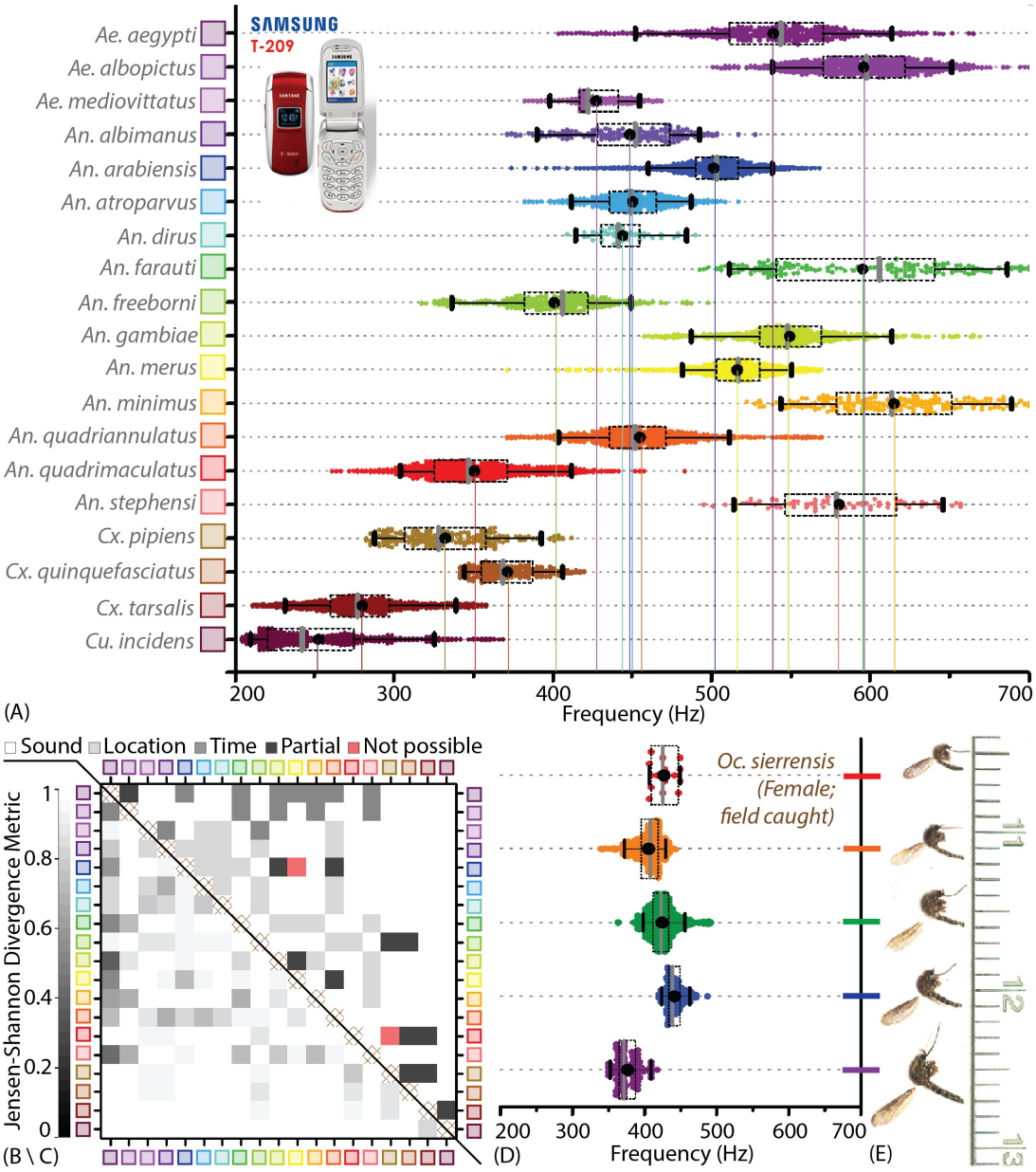

Fig. 4. Spatio-temporal activity of mosquitoes in the field can be mapped using crowd-sourced acoustic data from mobile phone users.

A, Sample spectrograms from female *Culex spp.* (top) and *Anopheles spp.* (bottom) mosquitoes captured in the field at Ranomafana village in Madagascar. **B**, Frequency distributions for field-caught *Culex spp.* and *Anopheles spp.* mosquitoes in Ranomafana, forming a reference for identification of recordings from either species at this field site. **C**, Map of Ranomafana village showing distribution of female *Culex spp.*, *Anopheles spp.*, and *Mansonia spp.* mosquitoes, from mobile phone data recorded by 10 volunteers over the approximately 1 km X 2 km area. Each square represents one recording, and black circles indicate locations where volunteers reported encountering no mosquitoes. The map shows a complementary spatial gradient from riverbank to hillside in the relative proportion of *Anopheles spp.* and *Culex spp.* mosquitoes. Further, mosquito hotspots are interspersed with points having a reported lack of mosquitoes, highlighting the potential importance of micro-factors such as the distribution of water and livestock. **D**, Spatio-temporal activity map for female *Oc. sierrensis* mosquitoes in the Big Basin Park field site, using data collected by 13 hikers recording mosquitoes with their personal mobile phones, over a 3-hour period in an approximately 4.5 km X 5.5 km area. Each brown square represents one *Oc. sierrensis* female recording, and black dots represent sites where hikers reported encountering no mosquitoes at all. (Inset top left) Temporal distribution of the overall mosquito activity data depicted in **(D)** based on recording timestamps, showing the rise and fall of activity in each hour of the field study.

Figure 4: Spatio-temporal activity of mosquitoes in the field can be mapped using crowdsourced acoustic data from mobile phone users

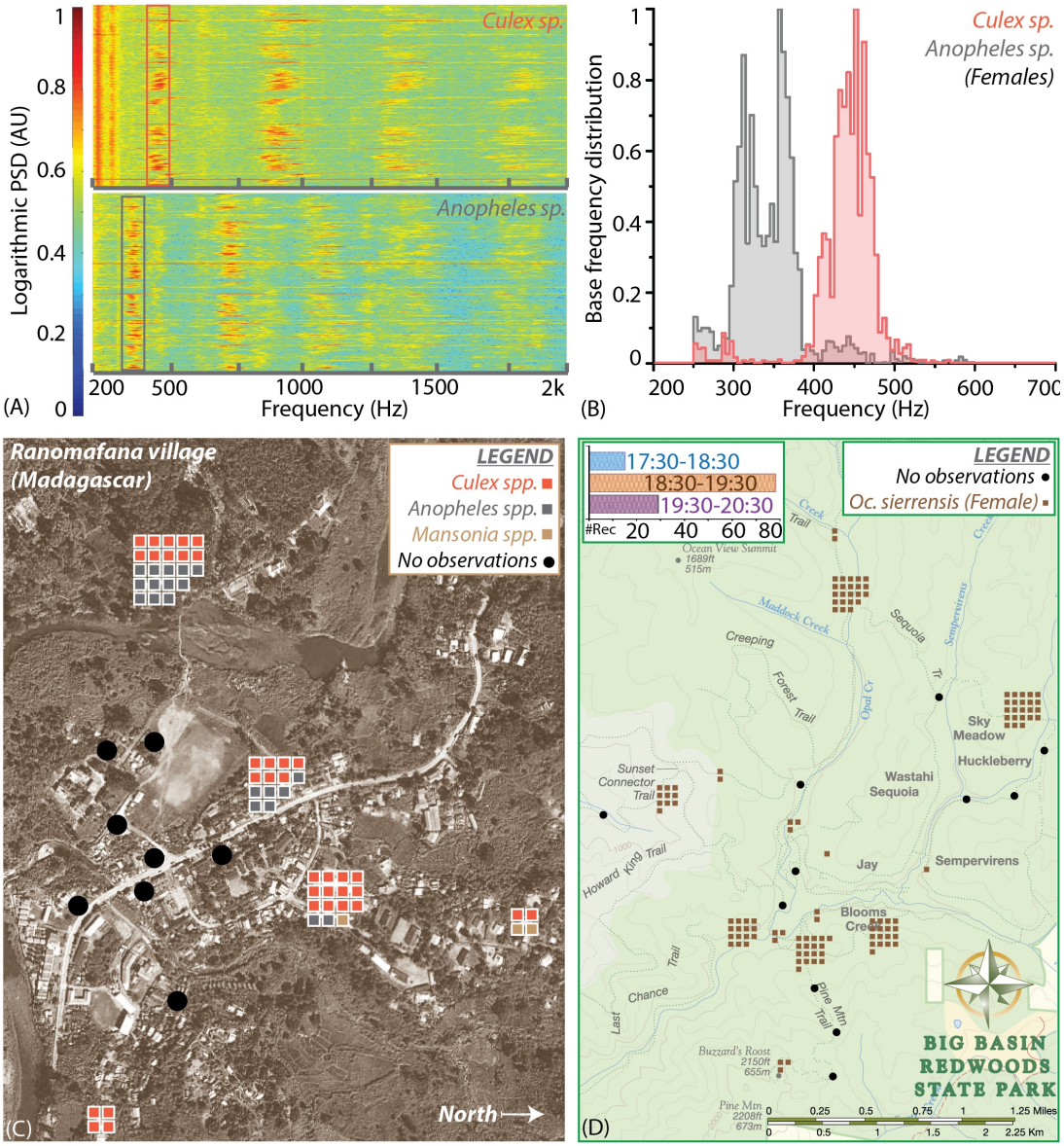

SUPPLEMENTARY INFORMATION

MATERIALS AND METHODS

Acquisition of acoustic data from mobile phones

Different mobile phones were used to collect sounds from mosquitoes, using audio recording software that was already freely available on the devices, including applications for voice messaging, voice memos, or sound recording. To locate the primary microphone on the body of the mobile phone, we either read the location off a user manual showing its different components, or found the microphone by trial-and-error, where we tapped the phone periphery and observed the response of the recording software to locate the area with maximum audio sensitivity. The primary microphone is oriented towards the mosquito for maximum sensitivity in audio acquisition. Audio data from the phones was compiled and transferred to a server for processing. This method applies to all figures.

Processing of acoustic data from mobile phones

The audio signals from mosquitoes were acquired at different sampling rates ranging from 8 kHz to 44.1 kHz and a variety of file formats, depending on the mobile phones and the specific in-built or user-defined settings on the recording applications used to acquire the signal. When a raw signal was acquired from the phone, it was converted into the WAV format for convenience of processing, with sampling rate interpolated to 44.1 kHz if sampled at a lower rate. To reduce constant background noise in the signal, we used a spectral subtraction algorithm, with the fundamental principle of subtracting the actual or expected frequency content of pure noise from the spectrum of the noisy signal. Here, we identified the background using an automated algorithm as those spectral bands that are constant with almost zero variation in amplitude and frequency across the entire sound clip. To generate the audio frequency spectrum over different

instants of time, we applied the Short Time Fourier Transform (STFT ; Signal Processing Toolbox, MATLAB R2015B) to produce a spectrogram with resolutions of 5 Hz in frequency and 20 ms in time, having a high degree (90%) of overlap between windows to achieve a trade-off between sufficient frequency resolution and accurate localization of the signal in time.

Construction of wingbeat frequency distributions

Using the spectrogram, we construct histograms for the distribution of peak frequencies for mosquitoes of a given species. Once a sound was identified (either manually or using an automated code) as belonging to a mosquito of a given species, the lowest frequency corresponding to a local maximum in amplitude was detecting using a peak finding algorithm. For a single flight trace, a representative wingbeat frequency can be found by averaging the fundamental frequency over all time instants. However, the wingbeat frequency from a single continuous mosquito signal can vary over a range of about 100 Hz for a tethered mosquito, and over a few tens of Hz for mosquitoes in free-flight. To explore this natural variation in wingbeat frequency over the duration for an audio signal, we did not average this frequency over time, but instead focused on the instantaneous frequency computed in each 20 ms interval time window. Each time window was treated as an individual instance, and its fundamental frequency added to a histogram, to bring out the natural variations in wingbeat frequency within a single signal. Peak frequencies from all time windows are binned with a bin size of 5 Hz - the same frequency resolution imposed upon the spectrogram. This yields a histogram that captures the distribution of peak frequencies for that mosquito species, without making *a priori* assumptions about the nature of this distribution. For statistical computations, the histograms are normalized by the total number of instances such that the area under the distribution sums up to 1, yielding a discrete probability density distribution for wingbeat frequency. However, for ease of representation in figures, probability mass functions where the histogram counts are normalized relative to the

maximum number of counts in a single bin are shown, so that each histogram spans 0 to 1 on the y-axis. This method applies to all figures.

Statistical tests and metrics

Wingbeat frequency was represented as discrete probability density distributions, with the frequency binned into intervals of 5 Hz (the computational accuracy for frequency in our STFT analyses) and the area under the probability density distribution summing up to 1.

The peak frequency measured in each time window of the video or audio was treated as an individual sample, and the 2-sample T-test carried out using the MATLAB Statistics toolbox at a significance level of 1% for peak frequencies of the 165 time windows compared. The peak frequency samples measured from video and audio were tested to check if the distributions had highly similar mean and variance, indicating that they have been sampled from the same probability distribution function. This method applies to Fig. 2C.

The Bhattacharya overlap distance (BD) and Jensen-Shannon Divergence metric (JSD) were computed between pairs of wingbeat frequency distributions, where the number of counts of wingbeat frequency in each bin are normalized by the product of the total number of samples and the range of the independent variable (frequency, 200 to 700 Hz) to yield a probability density distribution with unit area under the curve. BD is calculated as the sum of the geometric mean of the two probability densities in each bin, ranging between a minimum of 0 for disparate non-overlapping distributions and a maximum of 1 for identical distributions. The JSD is calculated as the square root of the arithmetic mean of the Kullback-Leibler divergences of each distribution with respect to the other, for each pair of distributions considered. These methods apply to Figs. 2G,H, and Fig. 3B.

Mosquito specimens

Mosquito colonies were sourced from a number of different labs and facilities, including our own. Mosquitoes were typically chosen to be between 5 to 15 days, with all individuals in a colony aged within two days of each other. Females were typically mated but not bloodfed.

The lab reared colonies used in this work sourced from the BEI Resources Vector Resource collection were *Aedes aegypti* (strain COSTA RICA, provided by the Animal Flight Lab at UC Berkeley), *Aedes aegypti* (strain NEW ORLEANS, reared at CDC, Atlanta), *Aedes aegypti* healthy and infected with *D. immitis* (strain NEW ORLEANS, provided by the Zohdy Lab at Auburn University), *Aedes albopictus* (strain ALBOPICTUS, reared at CDC, Atlanta), *Anopheles albimanus* (strain STECLA, reared at CDC, Atlanta), *Anopheles arabiensis* (strain DONGOLA, reared at CDC, Atlanta), *Anopheles arabiensis* (strain RUFISQUE, reared at CDC, Atlanta), *Anopheles atroparvus* (strain EBRO, reared at CDC, Atlanta), *Anopheles dirus* (strain WRAIR2, reared at CDC, Atlanta), *Anopheles farauti* (strain FAR1, reared at CDC, Atlanta), *Anopheles freeborni* (strain F1, reared at CDC, Atlanta), *Anopheles gambiae* (strain KISUMU, reared at CDC, Atlanta), *Anopheles gambiae* (strain AKRON - bendiocarb resistant, reared at CDC, Atlanta), *Anopheles gambiae* (strain RSP - permethrin resistant, reared at CDC, Atlanta), *Anopheles merus* (strain MAF, reared at CDC, Atlanta), *Anopheles minimus* (strain MINIMUS1, reared at CDC, Atlanta), *Anopheles quadriannulatus* (strain SANQUA, reared at CDC, Atlanta), *Anopheles stephensi* (strain STE2, reared at CDC, Atlanta), *Anopheles stephensi* (strain STE2, provided by the Luckhart Lab at UC Davis), *Culex quinquefasciatus* (strain JHB, reared at CDC, Atlanta), *Culex tarsalis* (strain Yolo, reared by us).

Colonies caught in the field or bred from catches included *Aedes aegypti* (F1, Los Angeles, provided by the Coffey Lab at UC Davis), *Aedes aegypti* (F1, Puerto Rico, provided by the

Coffey Lab at UC Davis), *Aedes mediovittatus* (F0, provided by the Coffey Lab at UC Davis), *Anopheles quadrimaculatus* (F22, Alabama, provided by the Mathias Lab at Auburn University), *Culex pipiens pipiens* (provided by the Santa Clara Vector Control District), *Culex pipiens pipiens* (provided by the San Mateo Vector Control District), *Culex quinquefasciatus* (provided by the San Mateo Vector Control District). Wild mosquitoes captured by us in field trials include *Culiseta incidens* (captured at Jasper Ridge Biological Preserve, Stanford University, and in San Francisco), *Ochlerotatus sierrensis* (captured at Big Basin Redwoods State Park, California, USA), *Anopheles spp.*, *Culex spp.* and *Mansonia spp.* (captured at the Centre ValBio and Ranomafana village, Madagascar).

Comparisons with high speed videography

We acquired high speed video of tethered mosquitoes in the lab using a Phantom v1610 camera, at 10000 frames per second. Simultaneously, we made audio recordings using a mobile phone placed with the primary microphone 10 mm away and oriented towards the mosquito. Since the audio and video are completely independent as the camera does not talk to the phone, synchronization was achieved using a specially designed setup to produce a specific light and sound pattern. We connected a piezoelectric buzzer and an LED to the same pin of an Arduino, which we programmed to produce a square wave at 5000 Hz and 50% duty cycle for 500 ms, followed by a 500 ms pause, and then a square wave at 2000 Hz for 500 ms. This gave us four time points - the beginning and end of each waveform - to use for aligning the corresponding spectrograms from video and audio in time. The video data was thresholded and the area of the wing (which we recorded face on) was computed in each frame. We plotted a waveform of the change in projected wing area over time, and applied the STFT to produce a spectrogram. The fundamental frequency in the spectrogram corresponded to the wingbeat, with higher harmonics corresponding to subtler variations in wing kinematics such as wing deformation during

clap-and-fling. Acoustic data from the mobile phone was processed as described in the section above. The two spectrograms were computed to the same time and frequency resolutions of 5 Hz and 20 ms, and aligned in time based on the best match of the four points of synchronization. This method applies to Fig. 2B.

Comparisons to studio microphones

Comparison with an acoustic gold standard was achieved using the Marshall MXL991 and Apex 220 microphones, the latter of which is calibrated to have a flat frequency response between 100 and 1000 Hz. The two studio microphones were connected to a pre-amplifier (Onyx) with the gain set to its maximum value of -60dB, after ensuring that this would still avoid saturation. We carried out experiments to calibrate the sensitivity of mobile phones over distance using a standardized sound source - a piezoelectric buzzer ringing at 500 Hz, with its amplitude measured before every recording to be constant at 77dB at the edge of the buzzer disc. To compare the ability of mobile phones to record mosquito sounds, we recorded tethered male and female *Culex tarsalis* mosquitoes. We placed the microphones at an identical distance to the left of the mosquito as we placed the mobile phone primary microphone to its right, since waveforms produced by the two wings are assumed to be symmetrical. We synchronized recordings from all three sources using the times of initiation and cessation of wingbeat sound, with multiple flight traces in a single dataset. Using the amplitudes recorded by the Marshall MXL991 studio microphone which has a known $1/r^2$ drop in recorded amplitude, we deduced the actual amplitude produced by the mosquito in a given experiment, and standardized the corresponding mobile phone SNR for a uniform source amplitude of 45dB (which we measured to be a typical amplitude produced by a mosquito). Spectrograms constructed independently and aligned in time are shown in Fig. S1. These methods apply to Fig. 2C,D and Fig. S1.

Acoustic data collection in the lab from tethered mosquitoes

Individual sound traces for distance calibration experiments were collected from tethered mosquitoes. Individuals were aspirated out of the cage and knocked out with a puff of carbon dioxide. The wings were gently spread to move them out of the way, and a pipette tip was affixed to the scutum with a bead of low melting insect wax. The pipette tip was clamped in a stand, and the appropriate recording device - mobile phone, studio microphone or high speed camera - was clamped in another stand at the desired orientation and a specified distance away from the pipette tip as measured by a ruler. The legs of the mosquito are gently stimulated to induce a flight reflex, after which the wings beat for a period of a few seconds to minutes. This method applies to Fig. 2A,B,D,E.

Acoustic data collection in the lab from caged populations

Wingbeat frequency distributions for a given species were measured from lab-reared populations maintained in 1-ft cubical cages. Cages typically contained between 100 to 300 individuals of males and females each, with the sexes segregated into separate cages whenever possible. The mobile phones were inserted by hand through the stockinette sleeves of the cages, with the primary microphones oriented away from the hand, and moved to follow individual mosquitoes in flight or against walls or corners of the cage. Care was taken to avoid introducing noise from bumping against the cage surfaces or rubbing against the sleeve. Between 5 to 10 minutes of data was collected per cage, and high amplitude noise due to bumps was eliminated using an automated algorithm. This method applies to Fig. 2F, Fig. 3A and Fig. S2. In some cases, individual mosquitoes were introduced into an otherwise empty cage, to record free flight traces from a specific mosquito in the lab. This method applies to Fig. 4A,B.

Acoustic data collection in the field

Field acoustic data was collected in a variety of locations, including homes and gardens around San Francisco and Palo Alto, USA, at Stanford University's Jasper Ridge Biological Preserve, and around the Centre ValBio in Ranomafana, Madagascar. Mosquitoes were either followed with a phone during free flight around the user, or captured live in a Ziploc bag and subsequently recorded by putting the phone's primary microphone against the bag (while taking care not to introduce noise due to crumpling or brushing the bag surface). This method applies to Fig. S3. The pilot demonstrations of field recording and mapping of mosquitoes were organized with small teams of volunteers working in pairs, with 14 and 10 users respectively in Big Basin Redwoods State Park in California, USA (20 km^2, between 5.30 to 8.30PM on 17 August 2016), and in Ranomafana village, district Ifanadiana, Madagascar (4 km^2, between 6PM and 8PM on 26-28 October 2016). During the studies, volunteers were hiking along trails in Big Basin Park, and were gathered in houses or shops in Ranomafana village. Prior to the field study, we initially collected live mosquitoes from the field, recorded them in the lab to create a curated database of signatures for those specific locations, and later morphologically identified them through microscopy for association with each acoustic signature (Fig. S4). Subsequently, field recordings were made by the teams, and each recording was assigned a species by comparing with the databases (Fig. S3). During the field exercises, the users also collected matched physical specimens from the field in grinder tubes and Ziploc bags corresponding to many of the audio recordings, which were morphologically identified to confirm the IDs assigned based on the acoustic database. The recordings were associated with a location as reported by GPS or the user, and timestamped automatically by the recording application on the mobile phone, for spatio-temporal placement of each observation. Maps were prepared by counting the number of reliably identified acoustic signatures for each location. This method applies to Fig. 4C,D.

Fig. S1. Schematic of proposed surveillance system using crowdsourced acoustic data from mobile phones

System architecture showing the collection of data by individual mobile phone users, processing to identify species of interest, and compilation into a map of mosquito activity. The diagram is depicted centering around data collection at a field site designated Location X. **A-D** occur prior to mobile phone based data collection, and represent steps required to enable crowdsourced acoustic surveillance at the field location. **A**, The mosquito population in the field at Location X is sampled, either by users in Ziploc bags or by using methods such as trapping, and live specimens characteristic to the location are collected. **B**, Wingbeat sounds of these field collected mosquitoes are recorded, with an acoustic dataset associated with each individual specimen. **C**, Specimens are identified to the genus (and preferably species) level by a method such as morphological ID through optical microscopy, or molecular ID through PCR. **D**, Acoustic data is processed and associated with specimen IDs to yield frequency distributions characteristic of the prevalent species in that field location, forming a reference database of mosquito sounds specific to Location X. **E-H** represent the proposed method for mobile phone based acoustic surveillance at the field location, assuming that the reference database of mosquito sound is already in place. **E**, Mosquitoes are recorded in the field by a user with a mobile phone, and the audio file together with metadata is compiled into a database for processing. **F**, The acoustic signals are processed to extract the frequencies present in the recorded mosquito sound. **G**, The computed acoustic spectrum and metadata obtained from the mobile phone are compared to the reference database for that location, and the most likely species corresponding to the computed frequency is identified. **H**, The identified species from this observation, together with the time and location metadata, are mapped back to the field Location X. This closes the loop for mobile phone based acoustic surveillance, from crowdsourced recorded data to information on spatio-temporal mosquito activity.

Figure 5: Schematic of proposed surveillance system using crowdsourced acoustic data from mobile phones

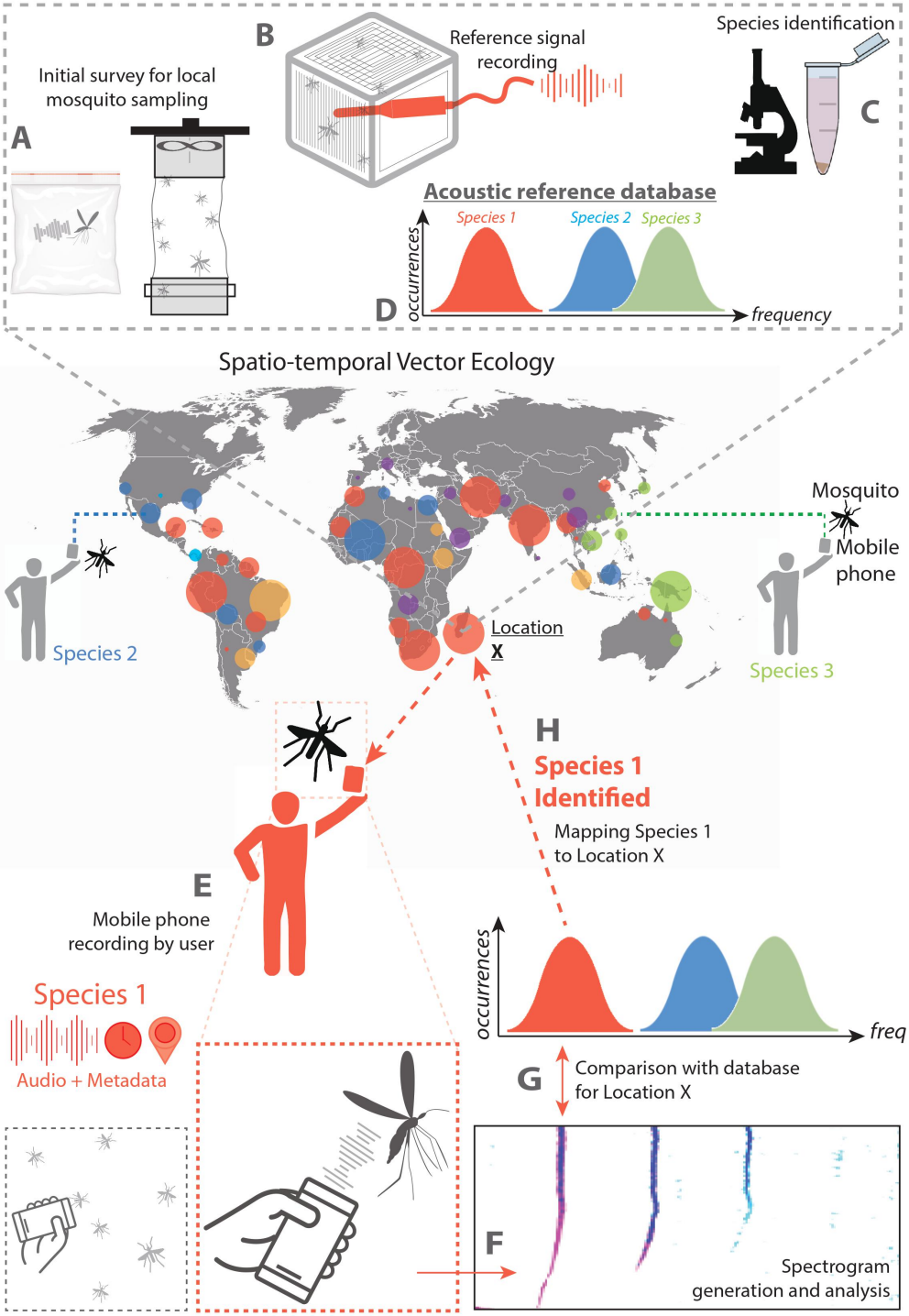

Fig. S2. Synchronized recordings of tethered mosquitoes using studio and mobile phone microphones shows exact correspondence at near-field distances below 50 mm

A-E, Comparison of power spectral density for synchronized simultaneous recordings of individual *Culex tarsalis* female mosquitoes using the MXL 991 studio microphone, the Apex 220 reference microphone and a mobile phone, taken at varying distances. The left column corresponds to the SGH T-209 feature phone, the middle column to the iPhone 4S iOS smartphone, and the right column to the Xperia Z3 Compact Android smartphone. **A**, Superimposed averaged spectra show that all phones acquire wingbeat sound at a high signal-to-noise ratio at 10 mm away from the mosquito. **B,C,D**, Overlaid spectrograms synchronized to within 20 ms in time show a near-perfect spectral match of within 5 Hz at each time interval, for the mobile phone microphone (red channel), MXL 991 (green channel) and the Apex 200 (blue channel), shown together as RGB images with intensity of colour corresponding to variations in power spectral density. Mobile phones strongly acquire mosquito sounds at 10 mm or even 50 mm, but their sensitivity drops sharply at distances of 100 mm. **E**, Superimposed averaged spectra show that only the Xperia Z3 continues to acquire wingbeat sound at 100 mm away from the mosquito, albeit at low signal-to-noise ratio. The T209 feature phone picks up low frequency noise between 300 to 600 Hz that overwhelms the mosquito frequencies, the iPhone 4S has low noise acquisition throughout, and the Xperia Z3 picks up high frequency noise above 1 kHz that leaves the mosquito frequency band relatively unaffected.

Figure 6: Synchronized recordings of tethered mosquitoes using studio and mobile phone microphones shows exact correspondence at near-field distances below 50 mm

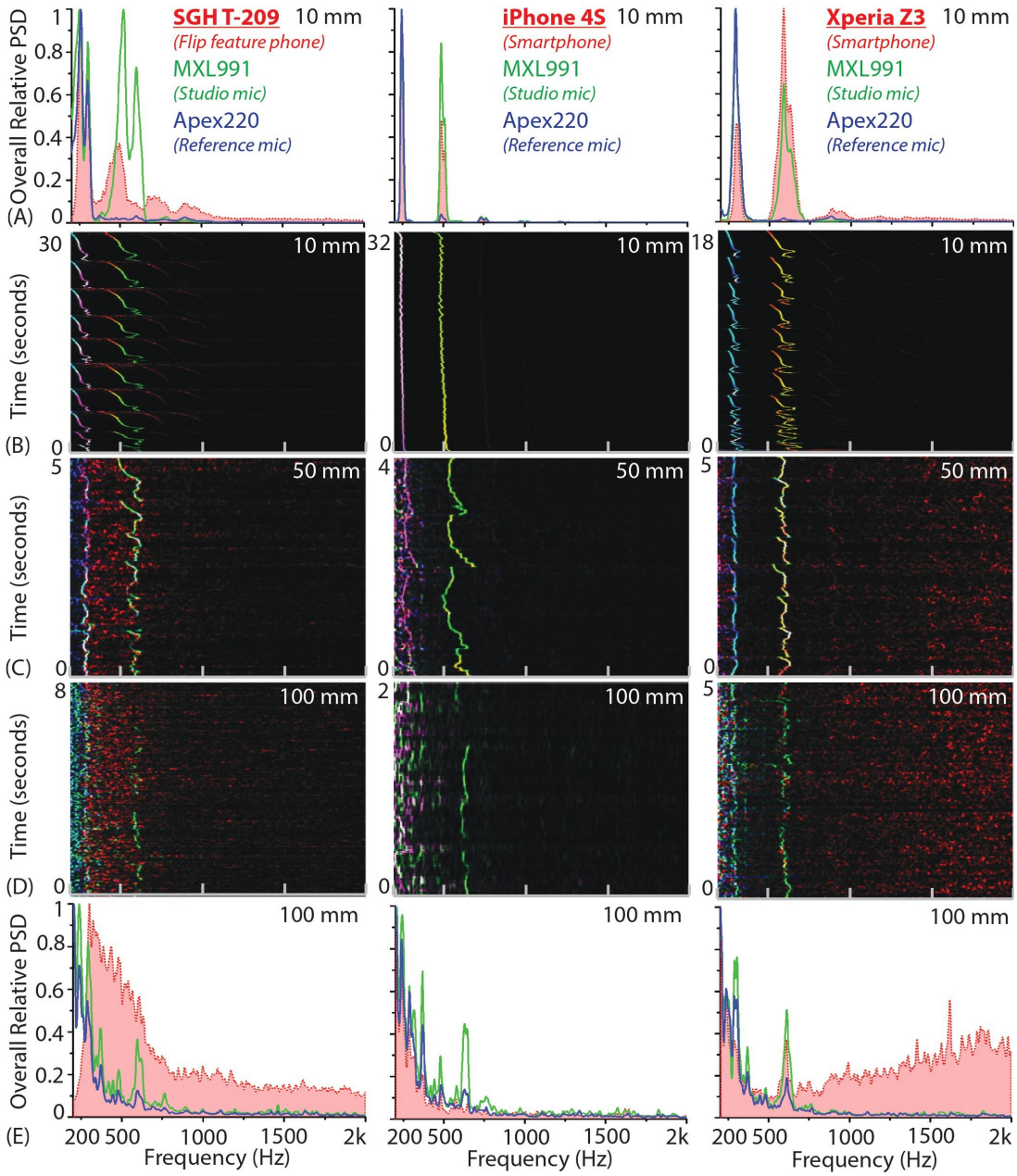

Fig. S3. Mosquito species can be distinguished with mobile phone acoustics and metadata **A-F**, Illustrative examples for distinguishing between medically relevant mosquito species using acoustics and metadata. All inset images of mosquito specimens are taken from Walter Reed Biosystematics Unit mosquito ID databases. **A**, Distinction by acoustic data alone - *Cx. pipiens* and *Anopheles gambiae*, which co-occur in many regions, can easily be distinguished by sound alone. **B**, Distinction by location metadata - *An. atroparvus* and *An. dirus* have overlapping acoustic spectra, but recordings are easily distinguished from each other by metadata pertaining to their distinct spatial distributions in Europe and South-East Asia respectively. **C**, Distinction by time metadata - *Aedes aegypti* and *An. gambiae* can occur together in many locations and have overlapping wingbeat frequency distributions, but can be easily distinguished by time of recording based on their diurnal and crepuscular biting habits respectively. **D**, Partial distinction by acoustic data - *Ae. aegypti* and *Ae. albopictus* have similar appearances, geographical distributions and biting habits in many areas. Although the wingbeat frequency distributions are not completely distinct, interquartile ranges do not overlap and a significant fraction of recordings can still be classified correctly as one or the other, making acoustic identification faster and easier than microscopy. Similarly in the case of *Cx. pipiens* and *Cx. quinquefasciatus*, which have partially distinguishable frequency spectra despite being otherwise indistinguishable except using PCR. **E**, Partial distinction by acoustic data - *An. arabiensis*, *An. gambiae*, and *An. quadriannulatus*, which are members of a species complex that are identical in appearance and often overlapping in habitat, have non-overlapping interquartile ranges for wingbeat frequency distributions implying that the majority of acoustic samples can be classified correctly as one among the three. **F**, *An. arabiensis* is indistinguishable based on mobile phone acoustic data from *An. merus*, another members of the *An. gambiae s.l.* species complex, exposing a relatively rare limitation of species identification using mobile phone acoustic surveillance.

Figure 7: Mosquito species can be distinguished with mobile phone acoustics and metadata

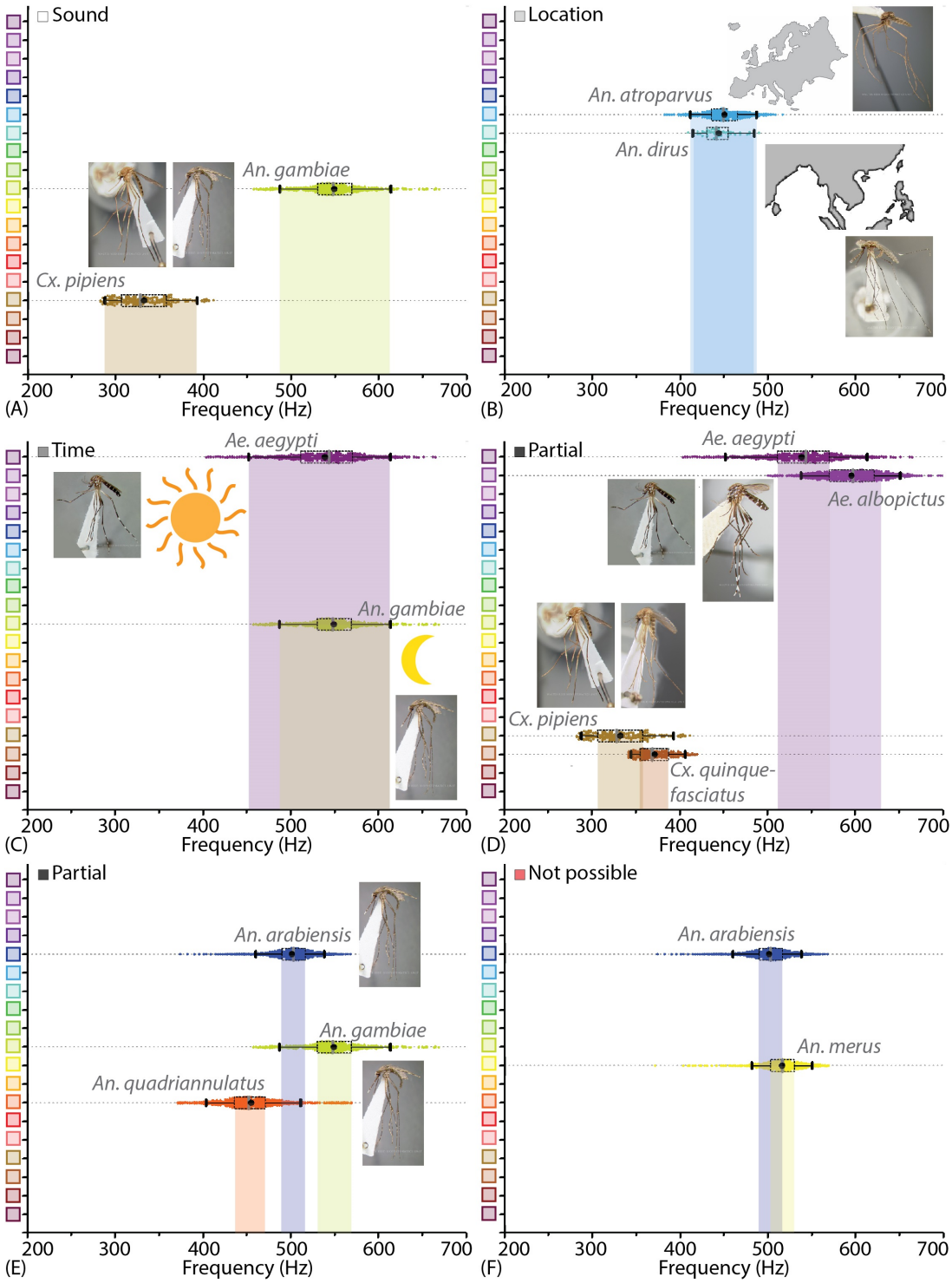

Fig. S4. Mobile phones are capable of acquiring mosquito sounds in a variety of field environments

A-F, Raw spectrograms of acoustic data acquired by various mobile phone users in different field conditions, with base frequencies of mosquito sounds highlighted by a box. The signals include sources of noise such as human speech, fire truck sirens, and birdsong, and were acquired in both urban **(A-D)** and forested **(E,F)** environments, including indoor **(A,B)** and outdoor **(C-F)** settings. Mosquitoes recorded were wither followed in free-flight **(A,C,E** or captured in a plastic ziploc bag prior to recording **(B,D,F)**. All spectrograms show raw spectra without background correction or noise removal, and show the spectra from extraneous acoustic sources (speech, sirens) to distinguish the characteristics of mosquito spectra from other sounds. Spectrograms **A-F** correspond to sounds in Supplementary Audio SA2-7.
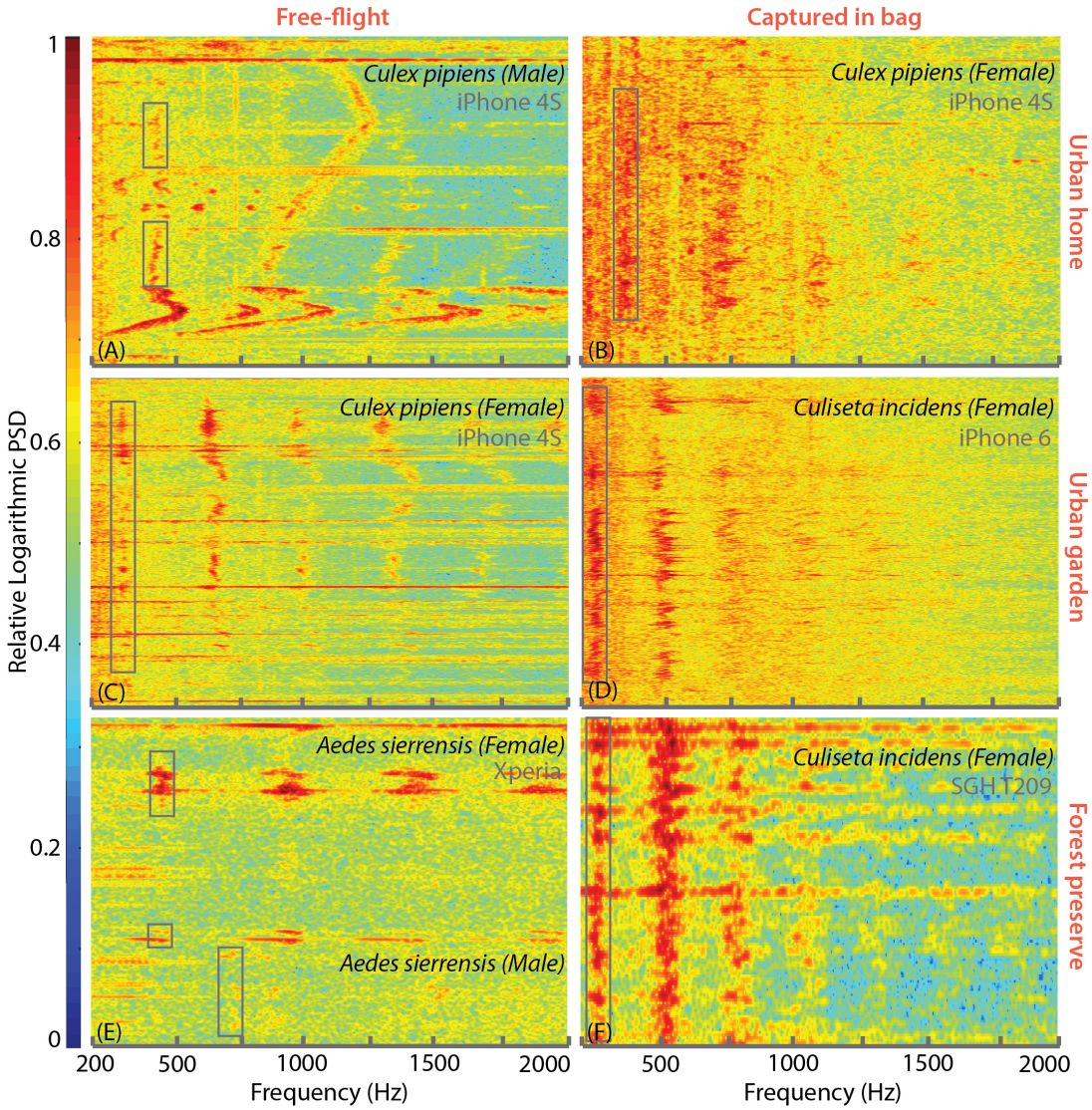
Figure 8: Mobile phones are capable of acquiring mosquito sounds in a variety of field environments